RESEARCH PROTOCOL

CORTICOLIMBIC DEGENERATION AND TREATMENT OF DEMENTIA

AUGUST 26, 2008

PRINCIPAL INVESTIGATOR

John G. Csernansky, M.D.
Gilman Professor and Chairman
Department of Psychiatry and Behavioral Sciences
Northwestern Feinberg School of Medicine
446 E. Ontario St., Suite 7-200
Chicago, Illinois 60611
Phone: (312) 926-2323
Fax: (312) 695-6276
E-mail: jgc@northwestern.edu

STUDY SITES

Data Collection
Washington University School of Medicine
Alzheimer's Disease Research Center (ADRC)
4488 Forest Park Ave #130
St. Louis, MO 63108

Data Analysis of De-identified Data
Northwestern University
Department of Psychiatry and Behavioral Sciences
446 E. Ontario, Suite 7-200
Chicago, IL 60611

TABLE OF CONTENTS

PURPOSE AND OBJECTIVES

Amyloid plaques, neurofibrillary tangles and other indications of neuronal degeneration in the hippocampus and cortical structures that are functionally related to it, such as the parahippocampal and cingulate gyri, are among the neuropathological hallmarks of AD (Hyman, et al, 1984 and 1987; Arnold, et al, 1991; Gomez-Isla, et al, 1996; Berg, et al, 1998). Since these corticolimbic structures have been shown in humans to play a critical role in declarative memory (Squire and Zola-Morgan, 1991), neurodegeneration within them has been hypothesized to be the basis for memory losses in patients with dementia of the Alzheimer type (DAT). Moreover, progressive structural degeneration of the hippocampus occurs in parallel with clinical worsening of the disease (Jobst, et al, 1994; Fox, et al, 1996; Jack, et al, 1998).

Treatment with cholinesterase inhibitors is now considered routine for patients with very mild-to-mild DAT (Knopman and Morris, 1997; Samuels and Davis, 1998). A number of cholinesterase inhibitors (e.g., tacrine, donepezil, rivastigmine, and galantamine) are commercially available, and there is ample evidence of their capacity to ameliorate cognitive deficits associated with AD (Corey-Bloom, et al, 1998; Davis, et al, 1992; Farlow, et al, 1992; Knapp,et al, 1994; Morris, et al, 1998; Rogers, et al, 1998; Rogers and Friedhoff, 1996; Thal, et al, 1996; Wilcock and Wilkinson, 1996). However, these studies provide little evidence that cholinesterase inhibitors have the capacity to alter the progression of the disease. Recently, the first drug treatment for DAT other than a cholinesterase inhibitor was approved for use in the U.S. Memantine, a voltage dependent, uncompetitive NMDA antagonist, has also been shown to ameliorate the cognitive deficits associated with AD (Reisberg, et al, 2003), and in a trial comparing combined memantine/donepezil treatment to donepezil alone, the combination of memantine and donepezil was demonstrated to have superior efficacy (Tariot, et al, 2004). Because the mechanism of action of this drug involves modulation of the potentially excitotoxic neurotransmitter, glutamate, it has been hypothesized that this drug may slow progression of the disease process in AD (Jarvis and Figgitt, 2003). However, there is no direct evidence of memantine's capacity to slow the progression of neurodegeneration in DAT patients.

During the initial funding period of this grant, we tested the hypothesis that the volume and shape of the hippocampus could predict the outcome of treatment with donepezil in patients with very mild-to-mild DAT. The rationale for this experiment was that hippocampal neurons receive cholinergic afferent projections (Umbriaco, et al, 1995), and so became the indirect targets of cholinomimetic treatments. We now propose to extend this investigation of the relationships between neuroanatomical structure and treatment response in patients with DAT by 1) determining what neuroanatomical changes are most strongly correlated with the progression of cognitive deficits in patients with DAT (*Specific Aim 1)*, and 2) determining whether treatment with cholinesterase inhibitors and/or adjunctive memantine can slow progression of the neuroanatomical and cognitive/behavioral changes associated with AD *(Specific Aim 2)*.

The specific aims and hypotheses of the project are as follows:

Specific Aim 1:

To determine what neuroanatomical measures are most strongly correlated with the progression of cognitive deficits in patients with DAT, we propose to use high resolution magnetic resonance (MR) imaging and the tools of computational anatomy to assess changes in the structure of the hippocampus, parahippocampal gyrus and cingulate gyrus in subjects with very mild-to-mild DAT over two years. During the first funding period of this project, we collected data using MR imaging and large-deformation high dimensional brain mapping (HDBM-LD) that shows that progressive hippocampal volume loss and shape change discriminates subjects with very mild DAT from nondemented controls (see Progress Report). The volume, thickness, and surface area of the parahippocampal and cingulate gyri will be assessed in the proposed work using labeled cortical depth mapping (LCDM), a new computational tool that was developed during the last funding period (see Progress Report). (**Hypothesis 1: Over two years, decreases in hippocampal and cortical volumes, thinning of the cingulate and parahippocampal cortices, and changes in hippocampal shape will be correlated with the rate of cognitive decline in subjects with very mild-to-mild DAT. Moreover, in a stepwise regression**

model, each of these variables will predict the rate of cognitive decline in DAT subjects independently of each other and independently of the effects of age, gender and apoE allelic status.)

Specific Aim 2:

To determine whether cholinesterase inhibitors and memantine can slow the progression of disease in DAT subjects, we will use HDBM-LD and LCDM to compare the rate of change in the neuroanatomical measures listed above in three groups – 1) untreated DAT subjects, 2) DAT subjects treated with donepezil alone, and 3) DAT subjects treated with the combination of donepezil and memantine. Past, present and future subjects recruited from the ADRC as well as the Memory Diagnostic Center (MDC) at Washington University will be used for this study, and the period of treatment will be two years. Due to ethical considerations (see Research Design and Methods), drug treatment will be naturalistic and open label. (**Hypothesis 2: The rate of decreasing hippocampal and cortical volumes, thinning of the cingulate and parahippocampal cortices, and changing hippocampal shape will be equal in DAT subjects that are untreated and in DAT subjects that are treated with donepezil alone, but greater than the rate of volume loss, thinning and hippocampal shape change in DAT subjects that are treated with the combination of donepezil and memantine.)**

BACKGROUND

Cholinesterase Inhibitors as Treatments for DAT

Several cholinesterase inhibitors are now commercially available for the treatment of DAT, and have been shown to have at least ameliorative effects on the symptoms of DAT, including memory loss (Corey-Bloom, et al, 1998; Davis, et al. 1992; Farlow, et al, 1992; Knapp,et al, 1994; Morris, et al, 1998; Rogers, et al., 1998; Rogers and Friedhoff, 1996; Thal, et al, 1996; Wilcock and Wilkinson, 1996). Cholinergic projections from the nucleus basalis are dispersed widely throughout the brain, and include the hippocampus, parahippocampal gyrus, cingulate gyrus and other neocortical areas. However, because of the central role played by the hippocampus and structures related to it in memory (Zola-Morgan and Squire, 1993), and the high frequency with which these structures are affected early in the course of Alzheimer's disease (Hyman, et al, 1984 and 1987; Arnold, et al, 1991; Gomez-Isla, et al, 1996; Berg, et al, 1998), these structures may be especially involved in symptom production and treatment response in subjects with DAT.

The precise mechanism of action of cholinesterase inhibitors for the treatment of DAT remains under investigation. Terminals for acetylcholine are found throughout the CA1 subfield of the hippocampus (Umbriaco, et al, 1995), and studies of neurotransmitter receptors show that the hippocampus contains a variety of receptors for acetylcholine. Receptors for both muscarinic (M1) and nicotinic ACh receptors are expressed throughout the CA1 subfield of the hippocampus. In particular, M1 receptors are found on the terminals of pyramidal neurons where they suppress excitatory activity (Dutar and Nicoll, 1988; Sheridan and Sutor, 1990), and on the terminals of inhibitory/GABA interneurons where they suppress GABA release (Behrends and Ten Bruggencate, 1993). However, while acetylcholine has various sites of action within the hippocampus, the net result of these effects appears to be the excitation of hippocampal pyramidal neurons (Steckler and Sahgal, 1995). In rats, injection of the prototypical cholinesterase inhibitor, physostigmine, directly into the hippocampus reverses the memory deficits induced by scopolamine (Ohno, et al, 1996). RU47213, another cholinesterase inhibitor, similarly reverses the working memory deficits of rats in the radial arm maze induced by scopolamine (M'Harzi, et al, 1997). These studies suggest that cholinomimetic drugs are effective in reversing cognitive deficits due to experimentally-induced cholinergic deficits.

Relatively few studies have addressed the question of whether treatment with cholinesterase inhibitors can slow the progression of the AD process. In many clinical studies of cholinesterase inhibitors in patients with DAT, improvements in cognition are only temporary and when declines in cognition resume, they proceed similarly in patients that have received active treatment and placebo (Burns, et al, 1999; Feldman, et al, 2001; Raskind, et al, 2000; Rogers, et al, 1998). Moreover, there is no obvious neural mechanism by which acetylcholine might exert neuroprotective effects. Instead, acetylcholine is generally considered to be an

excitatory neurotransmitter (Steckler and Sahgal, 1995), and elevations in the release of acetylcholine have even been reported to have neurotoxic effects (Kim, et al, 1999).

NMDA Antagonists as Treatments for DAT

Hippocampal pyramidal neurons are glutamatergic and are interconnected via a trisynaptic excitatory circuit (Wyss and van Groen, 1989). When experimentally-induced increases in the release of glutamate occur, ongoing destruction of the hippocampus can proceed through a cascade of excitotoxicity (Choi, et al, 1988; Lipton and Rosenberg, 1994). Of particular importance to the pathogenesis of AD and to the mechanism of action of memantine, Aβ may also initiate the excitotoxic cascade. For example, Harkany, et al (2000), reported that Aβ depolarizes astroglial membranes and blocks glutamate uptake by such cells. Increases in the resultant levels of glutamate then trigger neuronal damage, which is blocked by the non-competitive NMDA antagonist, MK-801. Barger and Basile (2001) have also suggested that glial cells may be a source of the glutamate released by Aβ. Excitotoxic stimulation, in turn, promotes the processing of APP so that more pathogenic forms of Aβ, such as $A\beta_{42}$, accumulate (Mattson, et al, 1993). Finally, Parks, et al (2001) and Ikezu, et al (2003) have shown that the NMDA antagonist, MK-801, blocks the release of reactive oxygen species triggered by Aβ.

Memantine is a voltage-dependent, uncompetitive antagonist at NMDA-type glutamate receptors that does not interfere with the physiological actions of glutamate required for learning and memory (see Kilpatrick and Tillbrook, 2002 and Jarvis and Figgitt, 2003 for review). Because of this unusual pharmacology, it is devoid of the anesthestic and psychotogenic effects that characterize non-competitive NMDA antagonists, such as phencyclidine and MK-801 (Frankiewicz, et al, 1996). Twenty years ago, memantine was observed to have alerting effects in comatose patients (Miltner, 1982), and more than 10 years ago, memantine was first investigated for use in patients with AD (Ditzler, 1991). Memantine's hypothesized mechanism of action as an anti-dementia drug is the use-dependent (i.e., voltage-dependent) blockade of NMDA receptors that mediate excitotoxicity (Erdo and Schafer, 1991; Weller, et al, 1993) and neuronal degeneration triggered by Aβ (Miguel-Hidelgo, et al, 2002). Also, memantine increases the expression of brain-derived neuroprotective factor (BDNF) and trkB in the mammalian brain (Marvanova, et al, 2001).

The efficacy of memantine in patients with DAT has been recently been demonstrated in a major multi-center study in the US (Reisberg, et al, 2003), and in the fall of 2003, memantine was approved for use in the U.S. as a treatment for DAT. Also, combination therapy of memantine and donepezil has been shown to be superior to treatment with donepezil alone (Farlow, et al, 2003; Tariot, et al, 2004). However, while reports of memantine's efficacy have been impressive, it remains uncertain as to whether the drug can alter the progression of AD (Reisberg, et al, 2003). The potential of memantine to alter the course of AD rests on its capacity to block excitotoxicity (Jarvis and Figgitt, 2003). However, clinical trials alone cannot provide conclusive evidence of its ability to block excitotoxic neurodegeneration and so alter the underlying disease process of AD (see Areosa and Sherriff, 2003 for review).

Neuroanatomical Measures as Markers of Disease Progression

Substantial volume losses in medial temporal lobe brain structures, such as the hippocampus, have been reported using manual analysis of MR scans in DAT subjects (Jack, et al, 1992; Pearlson, et al, 1992; Scheltens, et al, 1992; Ikeda, et al, 1994). These studies are consistent with the results of post-mortem studies, which demonstrate substantial neuronal loss in the same brain areas (Gomez-Isla, et al, 1996). Substantial volume losses in the hippocampus and parahippocampal gyrus are seen in people with even mild DAT, and the progression of such volume losses correlates with symptomatic worsening (Jobst, et al, 1994; Fox, et al, 1996; Killiany, et al, 1993; Jack, et al, 1998; Laakso, et al, 1996; Murphy, et al, 1993; Mungas, et al, 2002; Wang, et al, 2003). In fact, progression of hippocampal volume loss over time has been suggested as a method of discriminating patients with DAT from patients with normal aging and other brain diseases (Fox, et al, 1996;

Jack, et al, 1998). However, to date, there have been no studies that have answered the question of whether drug treatment alters the progression of neuroanatomical changes in patients with DAT.

Computerized methods for MR image analysis are being increasingly applied to the problem of identifying early forms of AD and other neuropsychiatric diseases (Iosifescu, et al, 1997; Thompson, et al, 1997; Ashburner, et al, 2003). We have recently completed several studies of the hippocampus using one of these methods (i.e., HDBM-LD) in subjects with very mild DAT, showing that hippocampal shape and volume can be used to discriminate DAT and control subjects (Csernansky, et al, 2000; Wang, et al, 2003) and that antemortem hippocampal volume predicted post-mortem tangle density in the hippocampus (Csernansky, et al, 2004). The results of these studies indicate that subjects with very mild DAT symptoms have highly characteristic shape deformations of the hippocampus as well as substantial hippocampal volume losses. These methods also hold promise for improving our capacity to study disease progression in DAT patients during drug treatment. In drug treatment studies, one is chiefly interested in assessing the degree of change within individuals. This problem is ideally addressed by methods that can transform one MR scan (i.e., at baseline) onto another (i.e., after drug treatment), thus quantifying subtle changes in neuroanatomical volumes and shapes. Fox and colleagues have performed a number of studies of this kind in subjects with and without DAT using a methodology called voxel compression mapping (VBM) (Fox, et al, 1996 and 2001; Fox and Freeborough, 1997; Freeborough and Fox, 1998). Also, this group has shown compelling evidence that VBM as compared to conventional manual volumetry significantly reduces the sample size required to detect the effects of drug treatment in patients with DAT (Fox, et al, 2000). During the first funding period of this project, we used HDBM-LD to compare patterns of change in hippocampal volume and shape in untreated patients with very mild DAT and non-demented controls (Wang, et al, 2003). In this study, we demonstrated that hippocampal shape change and the rate of volume loss provided complementary information for distinguishing subjects with DAT from the non-demented controls.

Clinical Significance of the Proposed Studies

There are two major areas of clinical significance to the proposed studies. First, the human study proposed in this application represent direct tests of the capacity of memantine and donepezil to slow the progression of DAT in patients. Second, we will be able to identify neuroanatomical measures that are most highly correlated for assessing the clinical progression of the AD process. By identifying neuroanatomical measures that are most sensitive to disease progression and to the potential effects of drug treatment, we will be identifying measures likely to be sensitive to the disease-altering effects of other therapeutic approaches to be developed in the future.

PRELIMINARY STUDIES

Discrimination of Subjects with Very Mild DAT and Controls Using Neuroanatomical Markers

To select neuroanatomical markers optimal for tracking the progression of disease in patients with DAT, one can first determine which neuroanatomical markers discriminate patients with early forms of DAT from controls. In our first study of this kind, we compared 18 subjects with very mild DAT and 18 elderly controls matched for age and gender using measures of hippocampal volume and shape generated by HDBM-LD (Csernansky, et al, 2000). The elderly subjects were categorized as having either very mild DAT (i.e. CDR 0.5) or no dementia (i.e., CDR 0) using the Clinical Dementia Rating Scale (CDR) (Morris, 1993). MR scans from a younger control group previously recruited for a study of schizophrenia (Csernansky, et al, 1998) were included so that we could also assess the effects of aging alone on hippocampal structure. Measures of hippocampal volume and shape both discriminated the CDR 0.5 and CDR 0 subjects. There was no significant difference in hippocampal volume between the elder non-demented subjects and the younger control subjects; however, the shape of the hippocampus also discriminated these two groups. Interestingly, the patterns of hippocampal shape deformation that discriminated CDR 0.5 and CDR 0 subjects and the CDR 0 subjects from younger controls were markedly different, indicating that the neurobiological effects of early DAT and healthy aging on hippocampal structure were distinct.

We have recently replicated the results of our first study of hippocampal structure in DAT in a larger, non-overlapping group of 46 subjects with DAT and 65 non-demented controls (Csernansky, et al, in preparation). The DAT and non-demented subjects were again matched with regard to gender (20/26 [m/f] for the DAT subjects and 19/46 [m/f] for the non-demented subjects) and age (mean (SD) 74.6 (7.9) years for the DAT subjects and 78.2 (7.7) years for the non-demented subjects). The mean (SD) sum-of-box score derived from the CDR was 4.05 (2.04) for the DAT subjects, indicating that the subjects had very mild-to-mild dementia. The non-demented subjects had a mean (SD) hippocampal volume of 2142 mm^3 (344) on the left and 2588 mm^3 (416) on the right, while the DAT subjects had a mean (SD) hippocampal volume of 1833 mm^3 (359) on the left and 2242 mm^3 (462) on the right.

Analysis of variance (ANOVA) showed that the difference in hippocampal volumes between these two subject groups was highly significant ($F = 21.38$, $df = 1,109$, $p < .0001$). As in our first study (Csernansky, et al, 2000), the difference in hippocampal shape between the two groups was evaluated using eigenvectors derived from the HDBM-LD transformations (see Research Design and Methods for further explanation). The first 20 eigenvectors explained 87.5% of the variance in hippocampal shape, and a MANOVA using these variables revealed a significant group difference ($F = 3.34$, $df = 20,90$, $p < .0001$). Moreover, in a "leave-one-out" (jackknife) discriminant function analysis, 56 of the 65 non-demented subjects (86% sensitivity) and 36 of 46 DAT subjects could be correctly classified (78% specificity). In this study, the group discrimination achieved by hippo-campal shape information alone was equivalent to the discrimination achieved when both hippocampal volume and shape information was used. Not surprisingly, eigenvector 1 was correlated with both left (rho = .69, $p < .0001$) and right (rho = .69, $p < .0001$) hippocampal volumes.

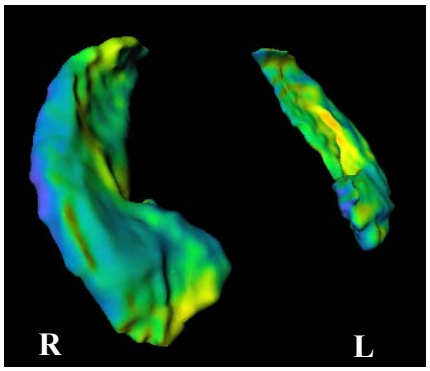

Figure 1. Visualizing the pattern of hippocampal surface deformation associated with DAT. The left and right hippocampi are viewed from above and to the right of the paired structures. The structure seen represents the composite hippocampus of the non-demented subjects and the shading indicates the degree of displacement of the hippocampal surface that was present in the DAT subjects (cooler colors (e.g. blue) represent inward deformation and warmer colors represent outward deformation). Areas of blue shading indicate regions of the hippocampal surface where there is localized volume loss (i.e., inward deformation) in the DAT subjects.

The pattern of hippocampal shape abnormality found in these DAT subjects (see Figure 1) was highly similar to the pattern of deformity we observed in our first study (Csernansky, et al, 2000), and again showed inward deformation of the head and lateral prominence of the hippocampus. This pattern of hippocampal deformation is highly consistent with patterns of plaque and tangle deposition in the CA1 hippocampal subfield observed in post-mortem studies of AD (Arnold, et al, 1991; Price and Morris, 1999).

Assessment of Disease Progression Using Neuroanatomical Markers

During the first funding period, we completed a longitudinal study comparing changes in hippocampal structure in CDR 0.5 and CDR 0 subjects matched for age and gender over approximately two years (mean interval in years (range) - CDR 0.5 – 2.0 (1.0-2.6) and CDR 0 subjects– 2.2 (1.4-4.1) (Wang, et al, 2003). The results of this study are critical for this application, as they demonstrate that our approach to assessing disease progression can discriminate between subjects with and without DAT, and so may also be sensitive to differences between groups of DAT patients treated with different drugs. This study included 18 CDR 0.5 subjects and 26 CDR 0 subjects that were partially overlapping with the subjects included in our previously published cross-sectional study (Csernansky, et al, 2000). The 18 CDR 0.5 subjects were not treated with cholinesterase inhibitors or memantine during the period of study. Measures of hippocampal shape and

volume were generated across both groups and time as in the cross-sectional study. At baseline, the CDR 0 subjects had a mean (SD) hippocampal volume of 2081(354) mm^3 on the left side and 2600 (481) mm^3 on the right side, while the CDR 0.5 subjects had a mean hippocampal volume of 1717 (224 mm^3) on the left side and 2186 (370 mm^3) on the right side. At follow-up, the CDR 0 subjects showed a hippocampal volume reduction of 82 mm^3 on the left side and 142 mm^3 on the right side, while the CDR 0.5 subjects showed a hippocampal volume reduction of 164 mm^3 on the left side and 236 mm^3 on the right side. ANOVA indicated a significant group effect on the rate of hippocampal volume loss ($F = 7.81$, $df = 1,42$, $p = 0.008$). This difference persisted after covarying hippocampal volumes for total cerebral brain volume ($p = 0.007$), total intra-cranial volume ($p = 0.008$) and scan interval ($p = 0.015$).

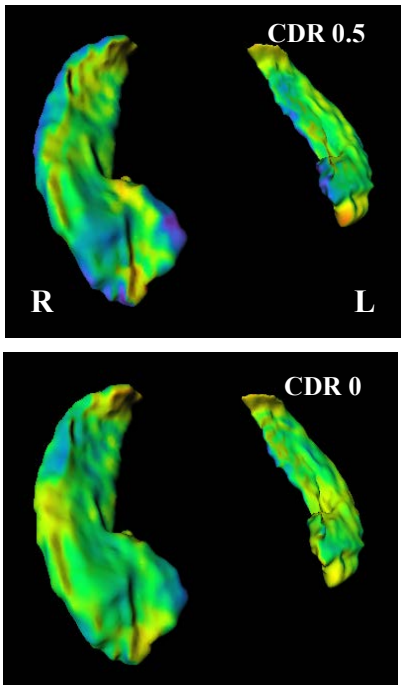

Figure 2. Comparisons from Baseline to Follow-up (two years) in CDR 0.5 and CDR 0 Elder Subjects. Displacement maps were used to visualize the across-time difference in hippocampal structure in the two subject groups. Cooler colors (blue to purple) signify areas of inward deformation over time. In the CDR 0.5 subjects, areas of inward deformation were more widespread and included more of the lateral edge of the hippocampus, while in the CDR 0 subjects, areas of inward deformation were smaller and confined to the head

There was also a group difference in the rate of progression of hippocampal shape deformity. The first 12 eigenvectors explained 75% of the variance in hippocampal shape, and using these 12 eigenvectors as variables in a MANOVA, we found a significant group effect ($F = 2.66$, $df = 12,31$, $p = 0.014$; effect size = 2.0). In a follow-up logistic regression analysis, the combination of eigenvectors 1, 2, 4, and 11 were found to be optimally useful for discriminating the patterns of hippocampal shape change in the two groups of subjects ($\chi^2 = 19.4$). Using these four eigenvectors, a significant group x time interaction was found ($F = 7.81$, $df = 4,39$, $p < 0.008$), and in a "take-one-out" discriminant function analysis, 22 out of 26 (84.6%) CDR 0 subjects and 15 out of 18 (83.3%) CDR 0.5 subjects were correctly classified. When hippocampal volume change was included in this logistic regression analysis, only eigenvectors 2, 4, and 11 were selected ($\chi^2=20.1$) (eigenvector 1 was again correlated with the change in hippocampal volume across subject groups - $r = -0.75$, $p < 0.0001$). Visualization of the changes in the shape of the hippocampus in the two groups revealed that areas of inward deformities over time were more widespread in the CDR 0.5 than in the CDR 0 subjects (see Figure 2).

Hippocampal Shape Predicts Response to Donepezil

A major objective during the first funding period was to test the hypothesis that an assessment of hippocampal structure could be used to predict the outcome of donepezil treatment in DAT patients. As proposed in our original application, estimates of cognitive decline over time were generated using CDR sum of-boxes scores, ADAS-Cog total scores, MMSE total scores and Neuropsychiatric Inventory (NPI) total scores (see Research Design and Methods section below for more description of these measures). Fifty-one subjects with DAT were included in this analysis and, to date, data were available for a minimum of 48 weeks in 38 subjects (this trial will be completed in the final year of the present funding period). In almost all cases, the subjects had been treated with donepezil, 10 mg/day, for the period of study – in rare subjects that could not tolerate this dose of donepezil, 5 mg/ day, was used. In addition, we included data from 65 non-demented subjects (CDR 0) in the analysis, so that we could evaluate variation in hippocampal shape related to drug response in the context of normative structure. To estimate the rate of annual change in the selected clinical measures, a slope value was calculated for each subject using a growth curve model (Laird and Ware, 1982). The mean (SD) annual rate of change for the sum-of-boxes scores was 0.13 (± 0.11, range -0.06 to +0.41) per year. Other mean (SD) annual rates of change were as follows: ADAS-Cog total score - 0.15 (± 0.29, range -0.29 to +1.32); MMSE total score - -0.084 (± 0.17, range - -0.61 to +0.16); the NPI total score - +0.027 (± 0.06, range -0.03 to +0.37). Thus, in general, mild deterioration was observed in the DAT subjects

treated with donepezil (i.e., slopes for sum-of-boxes scores, ADAS-Cog and NPI scores were positive, while MMSE slopes were negative).

Hippocampal volumes, total cerebral volumes and total intracranial volumes were not significantly correlated with any of the measures of cognitive decline. However, among the first 10 eigenvectors (which explained > 80% of the variance in hippocampal shape), eigenvector 3 coefficients were correlated with two measures of the rate of cognitive decline. More negative eigenvector 3 coefficient values were significantly correlated with increasing sum-of-boxes slope values ($r = -0.34$, $p = 0.03$, two-tailed) and with increasing NPI slope values ($r = -0.31$, $p = 0.05$, two-tailed). A trend correlation was observed between more negative eigenvector 3 coefficient values and decreasing MMSE total scores ($r = 0.29$, $p = 0.07$, two-tailed), but no correlation was observed between eigenvector 3 coefficient values and ADAS-Cog total scores ($r = -0.11$, $p = .50$, two-tailed). These correlations were unchanged after taking into account total cerebral brain volume, total intracranial volume, and age.

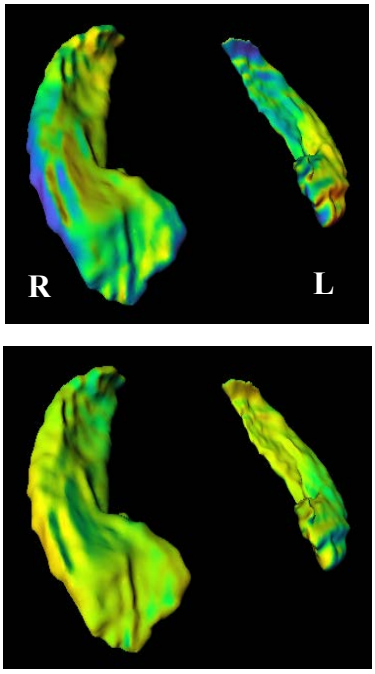

Figure 3. Pattern of Hippocampal Shape Variation Correlated with the Outcome of Donepezil Treatment.
The two panels illustrate the extremes of hippocampal shape variation in eigenvector 3, that were characteristic of DAT subjects who showed clinical worsening (top panel) and improvement (bottom panel) during donepezil treatment. Cooler colors (blue to purple) signify areas of inward deformation and warmer colors signify areas of outward deformation relative to the mean shape of all subjects.

The pattern of hippocampal shape variation represented by eigenvector 3 is shown in Figure 3. The pattern of shape variation associated with greater cognitive decline during donepezil treatment was similar to the pattern of shape deformation previously shown to discriminate CDR 0.5 and CDR 0 subjects (see Figure 1), and to be associated with disease progression changes CDR 0.5 subjects over time (see Figure 2) (i.e., inward deformation of the lateral prominence of the hippocampus). In turn, the relative absence of this pattern of deformation in hippocampal shape was associated a more favorable outcome during donepezil treatment. These results suggest that hippocampal shape may be a predictor of the capacity of DAT patients to respond to donepezil.

STUDY DESIGN

Clinical data and digital MR scans from the Specific Aims of this study will be de-identified and obtained for analysis from the clinical database maintained by the Alzheimer's Disease Research Center (ADRC) at Washington University via an electronically secure file transfer protocol (ftp). At Northwestern University, the data will be downloaded to a Pentium D based PC managed by Dr. Lei Wang. The data will be physically secure and will have continuous power via a UPS and connection to an emergency power supply. The NMFF's internet security system secures its network from the Internet via firewalls and a network intrusion detection system. Analysis of the data will be conducted by the Principle and Co-investigator. The confidentiality of the participants at Washington University will be protected as indicated in the "Code Access Agreement" signed by the PI and Washington University personnel such that Northwestern University personnel will not have access to subject identifiers or a master code list under any circumstances (see attached code access agreement).

Specific Aims 1& 2 - Monitoring Disease Progression During Treatment with Donepezil and Memantine in Subjects with Very Mild-to-Mild DAT

a. Overall Design and Source of Subjects.

Changes in specific neuroanatomical markers will be compared over a two year period in four groups of subjects – Group 1) subjects with very mild (CDR 0.5) to mild (CDR 1) DAT that are untreated with either cholinesterase inhibitors or memantine, Group 2) subjects with very mild (CDR 0.5) to mild (CDR 1) DAT that are treated with donepezil, Group 3) subjects with

very mild (CDR 0.5) to mild (CDR 1) DAT that are treated with the combination of donepezil and memantine, and Group 4) nondemented comparison subjects. MR scans and clinical data from Group 1 and Group 4 subjects will be obtained from the clinical database and MR image archive maintained by the ADRC at Washington University. The ADRC is directed by Dr. John Morris, who is also a Co-Investigator on this project. At present, repeat MR scans and clinical data are available for 21 Group 1 subjects and 44 Group 4 subjects. MR scans and clinical data from Group 2 subjects will be obtained from data collected during the initial funding period of this project. At present, complete sets of clinical data and repeat MR scans are available for 38 such subjects; however, 9 additional subjects are still completing the protocol – thus, the total number of Group 2 subjects could be as high as 47. Finally, repeat MR scans and clinical data from Group 3 subjects will be obtained during the proposed funding period of the project. Specifically, we propose to treat 50 new DAT subjects with the combination of memantine and donepezil during the proposed funding period, and again projecting an attrition rate of approximately 20% (see Data Analysis section below), this plan should yield approximately 40 Group 3 subjects for data analysis.

New subjects to be studied during the proposed funding period will be recruited from DAT patients enrolled at the Memory Diagnostic Center (MDC) at Washington University School of Medicine, also directed by Drs. John C. Morris and James Galvin. These subjects are referred to the MDC from community neurologists and from the ADRC at Washington University. Presently, MDC patients are prescribed donepezil as the cholinesterase inhibitor of first choice, because of its tolerability and ease of use (single daily dosing). Other cholinesterase inhibitors are offered only if the patient cannot tolerate donepezil or has a strong personal preference. A New Drug Application for memantine was submitted to the FDA in January of 2003, and memantine was approved for use in October, 2003. In February, 2003, the drug was distributed to U.S. pharmacies, and launch occurred in March, 2003. Thus, memantine will be clinically available in advance of the beginning of the proposed study. The MDC has evaluated the data available for memantine and plans to use this new drug almost exclusively as an adjunctive agent to donepezil (John Morris, M.D., personal communication).

Clinical diagnostic criteria for DAT at the ADRC and MDC at Washington University correspond to those established by the NINCDS-ADRDA Work Group (McKhann, et al, 1984), and have a 93% accuracy for the histopathological presence of AD at autopsy (Morris, et al, 1996; Berg, et al, 1998). All subjects are assessed annually using clinical, psychometric, and behavioral measures that are valid for the detection of very mild stages of DAT (Berg, et al, 1998). The clinical measures include staging of dementia severity using the CDR (Morris, 1993).

Treatment will be administered in this study in an open-label fashion. All DAT subjects selected for this study will already have been selected for donepezil therapy alone or the combination of donepezil and memantine, regardless of their participation in the proposed study. Therefore, randomization to a lesser form of drug therapy or placebo would be below the standard of care and therefore unethical (Kawas, et al, 1999; Knopman, et al, 1998). Also, by selecting subjects for this study who have already been identified as candidates for drug therapy, our sample should be representative of clinical populations prescribed such treatments.

All clinical evaluations will be performed blind to the results of neuroanatomical assessments. Therefore, no systematic bias will be introduced related to our main hypotheses involving correlations between the results of these biological assessments and treatment response. Subjects will be excluded from this study if they have already had a substantial period of treatment (i.e., more than 8 weeks) with a cholinesterase inhibitor. Vitamin E treatment (400-800 U/day), non-steroidal drugs and Cox-2 inhibitor drugs will be permitted during the treatment period, since this situation is typical of clinical settings in which cholinesterase inhibitors and memantine are administered, so long as the doses of these treatments remain constant throughout the treatment period. However, other drug treatments under investigation for their efficacy in DAT will not be permitted during the treatment period.

Prior to initiation of treatment, all subjects will undergo a comprehensive diagnostic evaluation using NINCDS-ADRDA criteria (McKhann, et al, 1984), as well as the CDR (Morris, 1993), the Alzheimer Disease Assessment Scale (ADAS; Rosen, et al, 1984), which includes a concise battery of cognitive tests (i.e., the ADAS-Cog), the Mini-Mental State Examination (MMSE; Folstein, et al, 1975), and the Neuropsychiatric Inventory (NPI), to assess the severity of dementia and behavioral symptoms related to dementia. Emergent

side-effects of donepezil and memantine treatment will be recorded using an instrument standard to clinical trials (Treatment Emergent Side-effect Scale [TESS]).

Drug treatment will begin with 5 mg/day of donepezil for six weeks. After six weeks of such treatment, the subjects' symptoms will be re-evaluated and any side-effects of treatment assessed and recorded. If no serious side-effects of donepezil are encountered, the dose of donepezil will be increased to 10 mg/day. For subjects prescribed the combination of donepezil and memantine, memantine (20 mg/day) will be added to the drug treatment regimen after the dose of donepezil has been established (i.e., at six weeks). Again, memantine will be initially started at 10 mg/day and increased to its full dose only if no serious side-effects are encountered. Subsequent evaluations will then be performed every 12 weeks for two years. All evaluations after 6 weeks will include the complete set of clinical and cognitive (i.e., ADAS-Cog) assessments, and a full diagnostic evaluation will be repeated annually (see Flowchart below). MR scans will be collected at baseline and after two years of treatment for all subjects who complete the entire period of treatment. For any subject that discontinues their participation in the study prematurely, the second MR scan will be collected at that time.

Clinical Trial Flowchart

Baseline	*Six Weeks*	*12 Weeks*	*Every 12 Weeks For Two Years*
Donepezil →→ → → → (5 mg/d)	Donepezil →→ → (5 to 10 mg/d)		
	Memantine →→ → (10 to 20 mg/d)		
Diagnosis			Repeat Diagnosis at 1 and 2 Yrs
CDR ADAS-Cog MMSE	CDR ADAS-Cog MMSE	CDR ADAS-Cog MMSE	CDR ADAS-Cog MMSE
NPI	NPI TESS	NPI TESS	NPI TESS
MRI			Repeat MRI at 2 Yrs

Subjects will be selected for this study if they meet NINCDS-ADRDA criteria for DAT at baseline (McKhann, et al, 1984), and have a score of 0.5 or 1 on the CDR (Morris, 1993). Subjects who no longer meet diagnostic criteria for DAT after one or two years of treatment, or who are diagnosed with another dementing illness, will still be followed for the remainder of the study, but their data will be evaluated separately from those subjects who continue to meet all inclusion and exclusion criteria. Based upon our prior experience with this population of subjects in the ADRC (Berg, et al, 1992), we expect such changes in diagnosis to be rare. The great majority of DAT subjects rated as 0.5 or 1 using the CDR are proven at autopsy to show the neuropathological signs of AD (Morris, et al, 1996; Berg, et al, 1998). Although it is possible that there will be subjects whose symptoms progress to the point where they can no longer be evaluated, this again should be rare given the demonstrated reliability and validity of the CDR across a wide range of severity of dementia symptoms (Berg, et al, 1992; Morris, et al, 1993).

Inclusion Criteria: 1) meets NINCDS-ADRDA criteria for DAT, 2) CDR score of 0.5 or 1, 3) 50-80 years of age, 4) able to give informed consent or has a primary caregiver or legal guardian, who can give informed consent.

Exclusion Criteria: 1) other psychiatric (e.g., depression) or neurological (e.g., CVA) disorders that would confound the assessment of dementia symptoms, 2) history of loss of consciousness, and 3) unstable or severe

medical illness (e.g., hepatotoxicity) that would make donepezil or memantine treatment or participation in other aspects of the study unsafe.

b. Selection of Instruments for Clinical Evaluation

Total sum-of-box scores from the CDR (Morris, 1993) will be used as the primary outcome measure. In our prior long-term studies (i.e., 4 to 10 years) of DAT subjects with very mild-to-mild DAT (i.e., CDR 0.5 to CDR 1), sum-of-boxes scores have been shown to be highly sensitive to disease progression and to have minimal ceiling or floor effects (Berg, et al, 1988; Berg, et al, 1992). In addition, so that the results of this study can be compared with large clinical treatment trials of DAT subjects, ADAS-Cog scores, total MMSE scores and total NPI scores will be used as secondary outcome measures (see below).

To perform the CDR, a clinician trained in its use rates the subject's cognitive abilities and function in *six* categories: memory, orientation, judgment and problem solving, community affairs, home and hobbies, and personal care. Impairment is rated 0-5 in the direction of increasing severity in each of these categories or *boxes*. The sum of these *box scores* is then compiled to yield CDR scores as follows: CDR 0 (no dementia); CDR 0.5 (very mild dementia); CDR 1 (mild dementia); CDR 2 (moderate dementia); and CDR 3 (severe dementia). Interrater reliability for the CDR is very high (Burke, et al, 1988), and subjects categorized with DAT over time using the CDR, including the CDR 0.5 category, are confirmed at autopsy as having AD with 96% accuracy (Morris, et al, 1988; Morris, et al, 1991; Berg and Morris, 1994). Clinicians at our Center all routinely receive extensive training in the use of the CDR, and interrater reliability is routinely monitored. Finally, sum-of-boxes scores have been shown to be a highly useful an index of dementia severity over time (Berg, et al, 1988; Berg, et al, 1992). In a study of 68 DAT subjects with beginning CDR scores of 0.5 or 1 followed for 4 to 10 years, sum-of-boxes scores declined in a relatively linear fashion and had very few ceiling or floor effects (i.e., all 68 DAT subjects could be rated using this measure at baseline and 24 months later) (Berg, et al, 1992).

As mentioned above, the ADAS-Cog (Rosen, et al, 1984), the MMSE total score (Folstein, et al, 1975), and the NPI will be used as secondary outcome measures. These measures have been previously used in treatment trials of DAT subjects as both primary and secondary measures of symptom severity, and have been demonstrated to be sensitive to the effects of cholinesterase inhibitors (Farlow, et al, 1998; Rogers, et al, 1996) and memantine (Reisberg, et al, 2003).

c. Neuroanatomical Rules for Brain Structure Boundaries

The hippocampus, parahippocampal gyrus and cingulate gyrus have been selected as the neuroanatomical variables to be assessed during the proposed funding period based on a review of the literature and our own prior results. Explicit neuroanatomical rules were used to define the boundaries of these brain structures. To generate templates, structural boundaries were outlined using semiautomated routines that combine autotracing and manual tracing techniques available in Analyze™. Analyze™ permits the simultaneous viewing of any point in the scan from three orthogonal planes. Autotracing functions encircle a selected region of uniform density by enclosing all contiguous pixels of similar density. The selection of tissue of a particular density is then achieved by setting thresholds that define the brightness of the pixels in the area of interest. Surrounding tissue of a different density (threshold) is deleted from the picture, leaving only the tissue of interest. When autotracing fails to segment tissues of similar density, the tissue is manually traced.

d. MR Scanning Protocols and Image Preprocessing

MR scans will be collected at the baseline assessment and after two years using a 1.5T VISION system (Siemens Medical Systems) with a UNIX based host computer (Sun Microsystems), actively shielded gradients, and echo-planar capability. Subjects will be positioned on the table with their canthomeatal line perpendicular to the table; head position stability is facilitated with adjustable cushioned head supports. A standardization object is placed in the field of view on the left side of the head for each MR scan. Prior to the scan, the

procedure is explained in detail to each subject, and techniques to tolerate small spaces and avoid claustrophobia are described. The MRI scans do not involve the administration of any contrast agent.

All MR scans will be acquired using a turbo-FLASH sequence (TR=20, TE=5.4, Flip angle=30^{o} ACQ-1, Matrix=256X256, Scanning time=13.5 minutes), that 3D datasets with 1 mm x 1 mm x 1 mm isotropic resolution across the entire cranium (Venkatesan and Haacke, 1997). A 2D set of proton density and T2 weighted images with standard 5-mm thicknesses will also be acquired for clinical interpretation of any unsuspected disease conditions, and to assess the number of white matter hyperintensities in each subject. Dr. Tom Conturo, Associate Professor of Radiology, oversees MR scan acquisition at Washington University School of Medicine, and together with his team, monitors scanner drift on a daily basis. Frequency, receiver gain, reference transmitter voltage, and signal-to-noise are examined. Phantoms of known dimensions are imaged and the gradient calibration is checked to make certain the correct size is registered. Protocols are also employed to check for ghosting artifacts. Further tests and calibration adjustments are performed when needed. Shims are used when needed to correct for field inhomogeneities.

For image analysis, the raw MR data are transferred to a SGI workstation at Washington University where 3D reconstructions of brains are obtained using Analyze^{TM} software (Rochester, MN). MR data files are identified by number only to maintain blind conditions for image analysis. Because the turbo-FLASH MR sequence yields 1 mm isotropic voxels, rescaling to correct discrepancies due to voxel isotropy is not necessary. Signed 16 bit MR datasets are compressed to unsigned 8 bit MR datasets by linearly rescaling the voxel intensities, such that voxels with intensity levels at two standard deviations above the white matter mean (corpus callosum) are mapped to 255, and voxels with intensity levels at two standard deviations below the CSF mean (third ventricle) are mapped to 0.

As a final step in the preprocessing of MR images, neuroanatomical landmarks are placed by Dr. Lei Wang. In each scan, twelve landmarks are placed at the external boundaries of the brain, and at the points where the anterior and posterior commissures intersect the midsagittal plane (Haller, et al, 1997). Additional landmarks are also placed at selected points along the principal axis of the hippocampus (Csernansky, et al, 1998).

i) *Hippocampus*. The most posterior slice containing the hippocampus is defined when the hippocampus first appears adjacent to the trigone of the lateral ventricle. A narrow band of gray matter along the medial aspect of the trigone opens to a thicker complex of gray matter and is separated from the trigone by a strip of white matter, i.e., the junction of the fimbria and fornix. The coronal slice shows an elongated gray matter shape because of the transverse orientation of the hippocampal tail. This complex is the cornu ammonis (CA), dentate gyrus and subiculum. It is difficult to select a point of separation between the CA and the subiculum because the superior component of the CA does not extend medially far enough to be the landmark of the medial border of the hippocampus, the inferior component of CA is continuous with the subiculum, and there is no gross anatomical separation of the subiculum, presubiculum, and parasubiculum, the lattermost being part of the parahippocampal gyrus. For these reasons, the subiculum and CA are combined in the volume called hippocampus, as has been done by others (Shenton, et al, 1992), and the inferior border of the CA-subiculum is continued medially with a straight horizontal line across the cortex of the parahippocampal gyrus. The cortex below this line is thus considered the parahippocampal gyrus, and the cortex above this line the hippocampus.

Progressing anteriorly from the tail, the orientation of the hippocampus changes from the medial-to-lateral alignment of the tail to the posterior-to-anterior alignment of the body. Thus, the body is cross-sectioned in the coronal slices perpendicular to its long axis, and appears to be divided by the white matter of the fimbria into a lower part that is the CA-subiculum and an upper part formed by the tail of the caudate nucleus. The thalamus appears medial and superior to the CA-subiculum complex.

The thalamus and caudate nucleus form the superior borders of the hippocampus in its posterior aspect. The white matter boundary (alveus and fimbria) between the hippocampus and caudate nucleus as well as any CSF lateral to the hippocampus is not included. The superior and lateral borders of the hippocampal body and head are identified by the contrast against the white matter or CSF. Vessels at the medial aspect of the hippocampus are excluded from the hippocampus. Where the amygdala appears at the superior boundary of the hippocampal head, it as well as the white matter boundary are excluded. However, the vertical digitation of the hippocampal

head which curves up and medial to the amygdala in coronal sections is included. The separation of the amygdala and hippocampus is best achieved by viewing sagittal and transverse sections.

ii) *Parahippocampal Gyrus (including entorhinal cortex).* Delineation of the structure is made primarily using MR slices oriented in the coronal plane, perpendicular to the AC-PC line. Posteriorly, the parahippocampal gyrus blends imperceptibly with the lingual gyrus of the occipital lobe. It is well known that temporo-occipital separation is not definable. Therefore, the posterior limit of the parahippocampal gyrus is defined as the anterior end of the calcarine sulcus. The same coronal section also defines the posterior limit of the cingulate gyrus, and the parahippocampal gyrus is situated between the notch of the calcarine sulcus below and the cingulate gyrus above.

Moving anteriorly, in coronal sections, the parahippocampal gyrus is limited by the subiculum medially and the collateral sulcus laterally. The anterior limit is defined by the rhinal sulcus which runs from lateral to medial, separating the parahippocampal gyrus from the temporal pole. The rhinal sulcus is identified in the axial section that shows the amygdala, head of hippocampus and uncal recess of the temporal horn. The sweep of the ambient gyrus over the medial aspect of amygdala in the axial section ends at a notch where the temporal pole begins. This notch is the rhinal sulcus. In coronal sections anterior to the amygdala, the superior limit of the parahippocampal gyrus is defined as the inflection point of the white matter at the inferior border of the gray matter of the amygdala.

iii) *Cingulate Gyrus.* The cingulate gyrus is delimited at its ventral aspect by the callosal sulcus, which separates it from the corpus callosum. Dorsally, it is delimited by the cingulate sulcus. Delineation of the structure is made primarily from MR slices oriented in the coronal plane, perpendicular to the AC-PC line.

The cingulate gyrus can be separated into anterior and posterior segments. The posterior limit of the anterior cingulate gyrus is taken to be in the coronal section perpendicular to the midpoint of the AC-PC line. As the cingulate gyrus extends anteriorly and wraps around the genu and rostrum of the corpus callosum, it tapers off gradually. Therefore, the anterior limit of the anterior cingulate gyrus is defined as the most rostral coronal section through the septum pellucidum, and the medial limit of the cingulate gyrus is the cortical surface in the interhemispheric fissure. The superior limit of the cingulate gyrus is the cortical surface forming the inferior bank of the cingulate sulcus (the superior bank being the superior frontal gyrus). This surface extends horizontally in a lateral direction to the fundus of the cingulate gyrus. At this point, a straight horizontal line is drawn through the thickness of the cortex to indicate the separation of the cingulate gyrus and superior frontal gyrus. From the lateral end of this horizontal line in the deep limit of the cortex, a straight line is drawn to the lateral limit of the cortex abutting the superior surface of the corpus callosum and separated from it by the callosal sulcus. The inferior limit of the cingulate gyrus is the inferior surface of the cortex forming the superior bank of the callosal surface (the inferior bank being the corpus callosum).

The posterior cingulate gyrus wraps around the splenium of the corpus callosum. In the coronal sections which run through the posterior end of thalamus, the anterior limit of the sub-splenium segment of the cingulate gyrus is defined as the most rostral extent through the anterior end of the calcarine sulcus. Indeed, the same coronal section also defines the posterior limit of the parahippocampal gyrus (see above). The posterior cingulate gyrus then starts at the anterior end of the calcarine sulcus, moving posteriorly, follow its bank until reaching the bifurcation point where the calcarine sulcus branches into the posterior calcarine sulcus and the parietal-occipital sulcus. A straight line is then drawn from this point upwards to the nearest point on the sub-parietal sulcus. The cortex below this line is also delineated as the cingulate gyrus. The posterior cingulate gyrus follows the bank of sub-parietal sulcus as it traces out a curve parallel to the corpus callosum (and the brain derma). The lateral extent of the posterior cingulate follows the upper bank of the calcarine sulcus.

e. Large Deformation High Dimensional Brain Mapping (HDBM-LD) to Assess the Volume and Shape of the Hippocampus

MR scans from different subject groups or from the same subject group at different points in time will be used to construct and compare composite volumes and shape representations. In statistical terms, these representations reflect the coordinate systems of the scans for the subject groups or time points that are associated with the smallest average squared error. In practical terms, these representations allow us to generate

automatic volume measurements of selected brain structures and to quantify neuroanatomical shapes. Composite representations for the subject groups are first created by forming the MR scans from the subject groups or time points into sets. Composite coordinate systems for the various sets of scans are then calculated by finding the correspondence of the coordinate system of each of the members of each group with a standard coordinate system. The composite coordinate system most representative of each population is then constructed from the average of these correspondences.

This approach relies fundamentally on our ability to calculate the correspondence of highly variable MR images with a common coordinate system. Since the earliest introduction of our brain mapping methods (Miller, et al, 1993; Christensen, et al, 1994; Grenander and Miller, 1994), we have studied the variability of mammalian brain anatomy by generating smooth correspondences (i.e. maps) from a single template onto families of target images. In our approach, the template represents the typical structure. Anatomical variation is then accommodated by performing transformations of the coordinate system of the template. The translation of every point in the template allows us to change the coordinate system in as many ways as there are points in the coordinate system (i.e. the number of voxels in the MR image). It is the high dimensionality of these transformations that differentiates our method from other mapping algorithms, and allows for the analysis of subtle characteristics of shape in small brain structures.

Our method uses a coarse-to-fine approach that fuses the elegant landmark work of Bookstein (Bookstein and Green, 1992; Bookstein, 1978) with the pioneering volume-based deformation work of Bajcsy and colleagues (Bajcsy, et al, 1983; Dann, et al, 1989), but extends these methods to accommodate local deformations so that the precise shape of brain structures can be studied. The importance of this innovation is that it allows neuroanatomists to embed information into brain maps that is optimally meaningful with regard to subtle anatomical variation. To help ensure that the transformations preserve key features of brain geometry (e.g. unbroken gyral surfaces), we force the transformations to obey physical laws of elasticity and fluidity. The continuum mechanics-based mathematical derivations that correspond to these constraints may be found in several previously published works (Grenander, et al, 1992; Miller, et al, 1993; Christensen, et al, 1994 and 1995; Grenander and Miller, 1994; Joshi, et al, 1997; Miller, et al, 1997).

There are limitations to any method, including HDBM-LD. First, our methods depend heavily on the quality of the gray scale image data. Currently, we are using the state-of-the-art high resolution MR images; however, as better resolution scanning sequences become available, we will employ them and very likely increase the precision of our assessments. Also, non-uniformities in the MR image data due to poor calibration and field inhomogeneities may result in mismatches of gray and white matter, because our current tools are not driven solely by information about geometric structure. We have worked hard to control these sources of error using conventional strategies. In addition, we have recently begun to develop transformation tools, which are driven solely by geometry and will therefore be invariant to non-uniformities in the MR images. Second, our methods are not entirely automatic, and the expertise of the expert neuroanatomist continues to play a key role. The expert creates the information in the template, and landmarks placed by experts may bias the initial manifold transformations. However, as regards the hippocampus, we have shown (see Haller, et al, 1997) that the transformations are robust to this potential source of error (i.e. the automatic results were more repeatable than the results obtained from manual outlining). Another potential limitation of our methods is that we make the assumption that the anatomies in the template and targets are diffeomorphic. Diffeomorphism can be roughly defined as the requirement that an analogous anatomical features can be found in every target and in the template. Moreover, as the transformations occur, the movements of contours and surfaces in the template never intersect. Thus, our mapping algorithms would currently fail if the template or the targets contained non-analogous features (e.g., tumor).

The quantification of hippocampal volume and shape using HDBM-LD begins with superimposing a triangulated graph of points onto the gray matter surface of the hippocampus within the template using a computer aided design program for fitting closed surfaces to connected subvolumes. This surface is then treated as a two-dimensional closed manifold and carried along as the template is transformed onto the target MR scans. When the transformations are completed, a vector field and the surface that it represents are generated for each selected brain structure in each of the target scans. Composite surfaces for each structure in each group of subjects are then produced by averaging the individual vector fields generated by the

transformations. Brain structure volumes are measured in the subject groups by calculating the gray matter volumes enclosed by the transformation-generated surfaces. Quantification of hippocampal shape is performed using the deformation vector fields produced by the transformations. A pooled covariance matrix is first computed using the vector fields from the transformed surfaces in all subjects. This covariance matrix is then reduced in its dimensionality by computing the complete orthonormal set of eigenvectors, and a subset of eigenvectors that accounts for ~75 % of the variance in hippocampal shape is used in group comparisons.

Recently, we have adapted these methods to specifically assess the rate of change in hippocampal shape over time (Wang, et al, 2003). From the pairs of MR images collected at different time points, the assessment of a change in the shape of the hippocampus over time is accomplished by mapping the transformations from the first time point onto the second time point via rigid-motion registration (rotation and translation). If no change in the shape of the hippocampus has occurred, the result of this transformation is an identity map (modulo rotation and translation). Conversely, any shape change that has occurred is defined as the deviation of the result of the transformation away from this identity map. To compare shape change in different groups of subjects, the covariance of the resulting transformation vector fields across all subjects is used, and shape change is assessed in each group by 1) obtaining a set of eigenvectors via the singular value decomposition of the covariance matrix, 2) computing coefficients associated with these eigenvectors for each subject, and 3) performing a MANOVA using the eigenvectors across all subjects. A post-hoc logistic regression is used to determine which of the eigenvectors are most discriminating of the groups being compared. Since the covariance of the shape change vector fields is empirical, repeat neuroanatomical data from nondemented (CDR 0) subjects are required in order to account for "normal" shape change during the analysis of shape change associated with DAT and its treatment.

f. Methods for Labeled Cortical Depth Mapping (LCDM) of the Parahippocampal and Cingulate Gyri

When the brain structure of interest is a subregion of the cerebral cortex (e.g., cingulate or parahippocampal gyrus), it is first necessary to create a segmentation of the various tissues (i.e., gray matter, white matter, and CSF) within that portion of the MR dataset, and in relationship to the geometry of the neocortex. We have recently developed specific algorithms for this purpose (see Figure 5).

Construction of the surface between gray and white matter then places us in a position to determine the probabilities of CSF, gray matter and white matter voxels within the segmented subvolume as a function of the closest distance from the voxel to this surface (see embedded surface represented by the yellow line in Figure 5, panel C). Specific algorithms to compute these distances were first developed in Miller, et al (2000), for several types of cortical subvolumes, and then refined by Ratnanather, et al (2003), for specific cortical regions. Figure 5, panel D shows an example of a profile that shows the probabilities of encountering CSF, gray matter and white matter voxels as a function of the distance to the gray matter/white matter surface in a single subject.

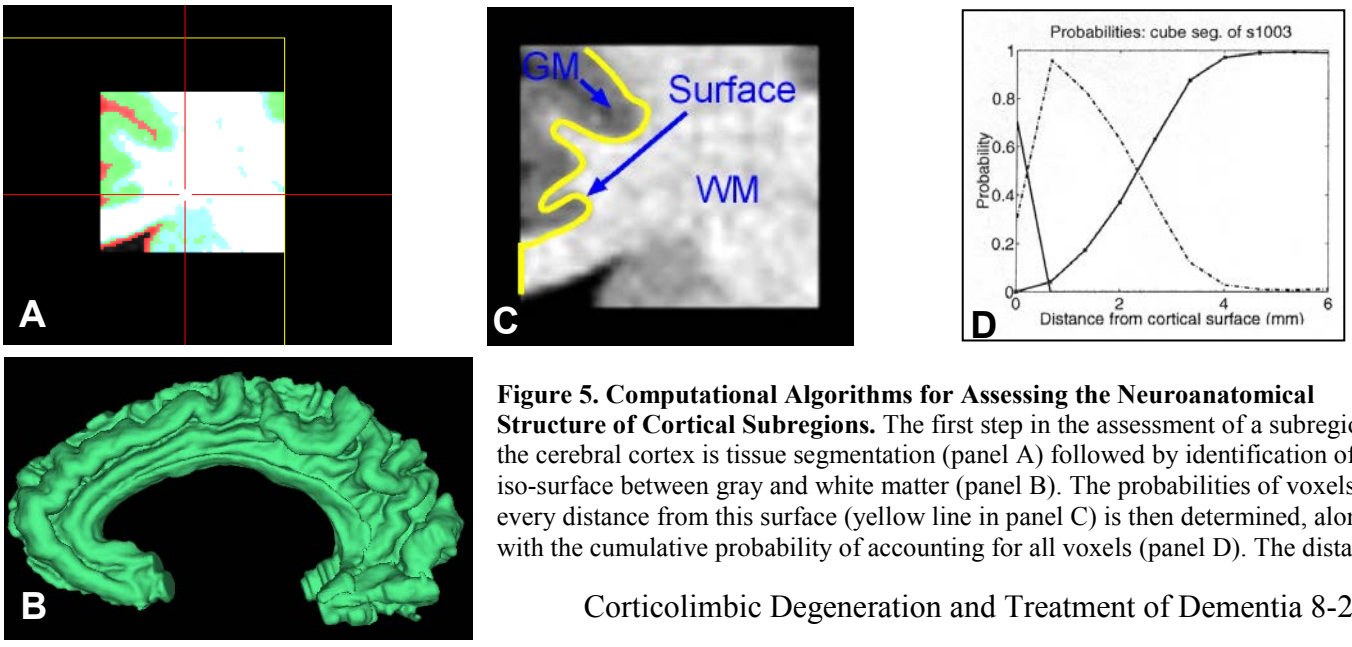

Figure 5. Computational Algorithms for Assessing the Neuroanatomical Structure of Cortical Subregions. The first step in the assessment of a subregion of the cerebral cortex is tissue segmentation (panel A) followed by identification of the iso-surface between gray and white matter (panel B). The probabilities of voxels at every distance from this surface (yellow line in panel C) is then determined, along with the cumulative probability of accounting for all voxels (panel D). The distance at

which a predetermined percentage of voxels are accounted for (e.g., 80%, 90%, etc.) can then be used as an estimate of cortical thickness across the region.

Cortical metrics such as gray matter volume and thickness are then generated from the probability profiles. The gray matter volume is equivalent to the cumulative sum of gray matter data in the profile. In turn, graymatter thickness is based on the distances from the gray matter/white matter surface where pre-assigned percentiles of voxels (e.g., 85%, 90% or 95%) are reached. Finally, gray matter surface area is computed by summing up all the triangles of the triangulated graph of the surface within the selected subvolume.

g. Assessment of Total Intracranial and Cerebral Volumes

Assessment of total intracranial and brain volumes is needed to control for generalized brain volume reduction, as has been reported by some investigators. Mathalon, et al (1993), have examined the issue of correction for head size and brain volume in such circumstances and shown that such corrections decrease unwanted variance while improving the ability to detect meaningful biological variation (e.g. correlations between brain structure volumes and age).

A template image is prepared by an expert using manual outlining techniques, and includes, in this case, segmentation data for the total intracranial and brain volumes. The entire MR image of the template is first globally registered with the MR image of each target using a landmark-based transformation and scalar points at the boundaries of the brain and in the midline. An elastic transformation (with eight basis vectors having 2187 basis coefficients) is then performed, which matches the templates for the total intracranial space and total brain to the target. As with the transformations developed to study the hippocampus, the manifold and the elastic transformations used for this measurement are concatenated together and all the anatomical features of the segmented template brain are carried through the transformation.

h. Data Analysis

To test **hypothesis 1** *(Decreases in hippocampal and cortical volumes, thinning of the cingulate and parahippocampal cortices, and changes in hippocampal shape will be correlated with the rate of cognitive decline in subjects with very mild-to-mild DAT.),* growth curve models will be developed to assess the rate of cognitive decline for the principal (i.e., CDR sum-of-boxes scores) and secondary (i.e., ADAS-cog total scores, MMSE total scores, and NPI total scores) outcome variables (Laird and Ware, 1982). The underlying framework for the Laird and Ware model is essentially the same as for a traditional univariate repeated measures analysis of variance (ANOVA). However, the traditional ANOVA framework is difficult to apply when assessments are not available for all subjects at all time points. We have previously examined the advantages and disadvantages of this statistical model in characterizing rates of cognitive decline in a group of CDR 0.5 and CDR 1 DAT subjects highly similar to the one recruited for this project (Berg, et al, 1992). The CDR sum-of-boxes score was found to be entirely adequate as an outcome variable in that analysis (Berg, et al, 1992), because of its minimal ceiling and floor effects. The Laird and Ware model generates a slope value and intercept (i.e., estimate of baseline severity) for each subject.

Variables to assess changes in structural volume, thickness, and shape (for the hippocampus) will be generated as described above. Bivariate correlations between changes in clinical and neuroanatomical variables will be estimated using non-parametric statistics (Spearman's rho). To assess whether observed bivariate relationships are independent of each other, a stepwise multiple regression model will be developed including all independent neuroanatomical variables and slope values for the CDR sum-of-boxes scores as the dependent variable.

To test **hypothesis 2** *(The rate of decreasing hippocampal and cortical volumes, thinning of the cingulate and parahippocampal cortices, and changing hippocampal shape will be equal in DAT subjects that are untreated and in DAT subjects that are treated with donepezil alone, but greater than the rate of volume loss, thinning and hippocampal shape change in DAT subjects that are treated with the combination of donepezil and*

memantine.), rates of change for the various neuroanatomical variables will be compared in DAT subjects that are untreated, that are treated with donepezil alone, that are treated with the combination of donepezil and memantine, and in nondemented comparison subjects. These analyses will be performed using simple difference scores (follow-up minus baseline) for volume and thickness variables. To compare rates of change in hippocampal shape across groups, a MANOVA using eigenvectors derived from the time 1-to-time 2 transformation covariance will be performed (see above). The distributional characteristics of each of these variables will be examined prior to hypothesis testing. Finally, non-parametric (Wilcoxon rank sum tests) statistics will be used to compare the groups.

i. Sample Size and Power Considerations

Based upon previous work by our group in similar groups of CDR 0.5 and CDR 1 DAT subjects (Berg, et al, 1988; Berg, et al, 1992), and on our experience with the subjects recruited and studied during the initial funding period, we estimate that the attrition rate of subjects who cannot continue in the study for the full two years due to pronounced deterioration, drug side-effects, or refusal to participate will be approximately 20% or less, leaving at least 40 subjects who would provide data for the entire two-year period. However, the number of subjects entered into the analysis may exceed this somewhat, since a slope value can be estimated for each subject who remains in the treatment trial for at least five assessments (one year). Estimating 40 subjects are used in the analysis used to test **Hypothesis 1**, we will have a power of .80 to detect a correlation (or partial correlation) of .44 or more with a 2-tailed significance level of .05 (Borenstein and Cohen, 1988; Kraemer and Thiemann, 1987).

For the testing of **Hypothesis 2**, we will be measuring the rate of change of neuroanatomical variables over time; therefore, the test-retest reliability for these variables must be high. To estimate the normative test-retest reliability of the neuroanatomical measures proposed in this application, we scanned eight healthy control subjects on two separate occasions approximately one month apart, and then estimated differences between volumes and surface contours of the hippocampus. At the first time point, the mean left hippocampal volume was 2,233 mm^3 and the mean right hippocampal volume was 2,699 mm^3; at the second time point, these volumes were 2,209 and 2,686 mm^3, respectively. Using repeated measures ANOVA, there were no significant test-retest differences in these volumes (on the left $F = .14$, $p = .72$; on the right $F = .07$, $p = .80$) and the intraclass correlation coefficient between these two datasets was very high (ICC = 0.93). To compare the similarity of surface contours at the two time points, we then registered all the scans with respect to the template and then calculated the percent overlap of voxels. The average percent overlap in the eight subjects was 87.4%, which is comparable to the overlap achieved by a single expert performing repeated manual segmentations of the hippocampus from the same MR scan (Haller, et al, 1997). To the test the reliability of shape assessment for the hippocampus, we generated the eigenvectors associated with this brain structure based on the eight control subjects at time point 1. The coefficients associated with these eigenvectors were then computed for each subject at both time 1 and time 2. The mean ICC for all eigenvector coefficients was very high - 0.89 (range of 0.83 to 0.94), suggesting very high repeatability. Finally, the standard deviation for the estimation of hippocampal volumes on the two occasions was 225 mm^3, and an annual rate of decrease in hippocampal volumes was 2 mm^3.

Assuming that the between-group effect size for comparisons of the rate of change of neuroanatomical variables is moderate (i.e., 0.5 or higher), and if the correlations in neuromorphometric measures within our proposed sample sizes at the different time points continue to be high (i.e., > .75), changes in brain structure shapes of the magnitude observed to date (see Progress Report and Wang, et al, 2003), and volume decreases of 50 mm^3 or greater over two years, would be detectable with greater than 85% power (Borenstein and Cohen, 1988; Kraemer and Thiemann, 1987).

HUMAN SUBJECTS

50 new subjects who meet NINDS-ADRDA criteria for probable AD (i.e. DAT), and who have been registered with the MDC for treatment will be recruited for participation in the project during the proposed

funding period. The age range of the subjects will be 50 to 80 years. Any subjects will be excluded if they have medical problems that would contraindicate treatment with donepezil or memantine or make administration of a MR scan or any other aspect of the protocol hazardous.

With regard to the inclusion of both genders and various minorities, the samples will be equally balanced for gender and include approximately 15% African-American subjects. This percentage is similar to the distribution of African-Americans who present to the ADRC and MDC. This distribution of subjects should also allow inclusion of gender as a covariate in data analyses.

2. Collected clinical data will include information about demographics, dementia symptoms, other behavioral disturbances, and performance on tests of cognition (i.e., the ADAS-Cog). In all cases, verbal or written information obtained directly from the patients and involved caregivers will be used. These evaluations will take place in an ordinary office setting. MR scan data will be collected according to established protocols at the Mallinckrodt Institute of Radiology at Washington University.

3. Patients will be recruited for participation in this project as they present to the MDC for assessment and treatment. Several neurologists work together to assess and treat patients at the MDC - Drs. Morris, Galvin, Holtzman, and Snider. As Director of the MDC and Co-Investigator on this project, Dr. Morris will work with the other treating neurologists to select possible subjects for this project. However, the consent of the individual treating neurologist, who has been informed of the goals and procedures of the project, and of the patients' families will always be obtained before any patient is approached to obtain their informed consent. For those patients who are incompetent to give informed consent, legal guardians will be approached to seek their informed consent for the subject's participation. All subjects shall give their ongoing assent for participation in the project, regardless of whether they have provided written informed consent as well.

4. The potential risks of this project include those associated with routine clinical interviews. The clinical interview and cognitive testing instruments to be used for the project could produce boredom and fatigue. However, breaks in interview sessions will be given whenever the subject requests or obvious fatigue is observed.

There are also risks in obtaining MRI scans. However, so long as subjects are properly screened to exclude individuals with metal embedded within their bodies, these risks are minimal and include feelings of claustrophobic fear while being scanned, and minor physical discomfort because of remaining still throughout the scanning procedure. Subjects will also be warned that should they have unremembered metal objects within their bodies, these objects could become heated by the radiofrequency energy of the scanner.

The risks of donepezil therapy include increased bowel movements, diarrhea, nausea, vomiting, dyspepsia, diminished appetite, and weight loss in approximately 10% of subjects. Less commonly, slight decreases in heart rate, insomnia, and psychomotor agitation have occurred. These side-effects can generally be managed by reducing the dose of donepezil from 10 to 5 mg/day. The side effects of memantine include diarrhea, insomnia, dizziness, headache, and rarely hallucinations. Also, as with any drug, idiocyncratic hypersensitivity reactions can rarely occur. Again, subjects will be warned about these risks, and excluded when they have a history of serious or unstable medical disorders.

5. To minimize these risks, clinical interviews and scanning sessions will be interrupted or discontinued if necessary. Subjects and their caregivers will also be carefully interviewed to exclude the possibility of including anyone with metal embedded in their body. Finally, all drug treatment will be performed in the context of an expert clinic. The DAT subjects will be closely monitored for any drug side-effects, and in subjects who experience such side-effects, the protocol will be discontinued. Personnel trained by the ADRC at Washington University in interviewing and testing DAT subjects will conduct all research-related procedures.

6. The risks of this project are relatively small, and not appreciably greater than the risks of ordinary inpatient assessment and non-invasive radiologic procedures. The drug treatment will be administered to these subjects in the context of ordinary clinical care in the MDC. If successful, knowledge may be gained about neuromorphometric predictors of treatment response in patients with DAT, and perhaps about the pathophysiology of AD in general. In consideration of the small risks and substantial scientific benefit of this work, we consider that risk/benefit ratio to be favorable.

7. All key personnel involved in the design or conduct of the research involving the human subjects will receive the required education on the protection of human research participants prior to funding of this project.

DATA MANAGEMENT

All data will be de-identified and then entered at Washington University. The Northwestern University research team will not have access to any identified data – all subjects in this study are given a random study number that will be used. All identifying data will be kept at Washington University. A distributed data entry system for this project will be used, with computers for data entry at all Washington University clinical data collection sites. Brain structure measures are entered into datasets using PC-type workstations. All computers currently use Excel data entry screens, formatted to simulate the hard copy data entry forms. All data are double-entered, and error checking programs are used to identify and correct errors. Once entered into these spreadsheets and checked, the data files are consolidated into the main SAS project database, which is maintained on a PC microcomputer under the direct supervision of Dr. Paul Thompson from Washington University, the project biostatistician. Back-ups are routinely performed to assure the preservation of the database. Data are checked for range, consistency, missing values, etc. Whenever errors are detected, reports are sent to the data entry sites, where the data are checked again.

Data entry system at Washington University is transitioning to a web-based data entry system for easier data management. This system uses SAS/IntrNet methods for data entry and formulates data entry tools using HTML screens (Thompson, 2003a, 2003b). This system integrates data entry with data analysis when necessary, and includes programs to check for completeness of data entry and other data monitoring tools to be run as data are entered, so that data evaluations and comparisons can be synchronous with data entry. This system is used on several other projects in which Dr. Thompson has management responsibilities, and is thus well tested and highly reliable.

The project database is maintained using SAS. Data from individual clinical or cognitive instruments are maintained in separate datasets, indexed by subject ID number, date and originating clinic. During data analysis, combined datasets are created as needed. Data are maintained in the master system datasets using a source/derived data approach, where source datasets are maintained unmodified, while the derived datasets are modified as needed. Thus, alterations that prove to be incorrect are easily rectified. The confidentiality of all data is maintained using the HIPPA compliance standards of Washington University. These standards involve retaining confidential information (name, address, telephone numbers, and social security number) in encrypted datasets or on removable media. No confidential information is posted to the web under any circumstances. All possible efforts are made to retain only the necessary information in all cases; that is, ID numbers are used in all possible cases, and actual identification information are used only when necessary and will not be included in the data that is transferred to Northwestern University.

Neuroimaging data produced by high dimensional transformations of the neuroanatomical template consists of volumes (in mm^3), symmetry metrics (no units), and shape metrics (e.g., individual eigenvector coefficient values). These data are also collected into Excel datasets, checked, and then merged into the project database.

As a first step in the data analysis process, exploratory data analyses will be undertaken for all neuroanatomical variables to assess their distributional properties and to identify outliers. Variables intended for use in MANOVA and other parametric analyses will be tested for deviations from distributional assumptions of the tests. If deviations are identified, we will attempt to find appropriate transformations, such as power or log transformations, which give the variables the required distributional properties. If no simple transformation can be used, alternative analyses with less rigid distributional requirements will be used. For example, rank-ordered group comparisons (e.g., Mann-Whitney U and Wilcoxon tests) and correlations (i.e. Spearman rho) may be used for ordered data for which we cannot demonstrate normality. Additionally, other methods (i.e., generalized estimating equations), which are compatible with other error distributions, will be considered.

REFERENCES

Areosa SA, Sherriff F. (2003) Memantine for dementia. Cochrane Database Syst Rev 1:CD003154.

Arnold SE, Hyman BT, Flory J, Damasio AR, Hoesen GW (1991) The topological and neuroanatomical distribution of neurofibrillary tangles and neuritic plaques in the cerebral cortex of patients with Alzheimer's disease. Cerebral Cortex 1:103-116.

Ashburner J, Csernansky JG, Davatzikos C, et al. (2003) Computer-assisted imaging to assess brain structure in healthy and diseased brains. Lancet: Neurology 2:79-88.

Bajcsy R, Lieberson R, Reivich M. (1983) A computerized system for the elastic matching of deformed radiographic images to idealized atlas images. J Comp Assisted Tomography 7:618-625.

Bardgett ME, Jackson JL, Taylor BM, Csernansky JG. (1998) The effects of kainic acid lesions on locomotor responses to haloperidol and clozapine. Psychopharmacology, 135:270-278.

Bardgett ME, Jacobs PS, Jackson JL, Csernansky JG. (1997). Kainic acid lesions enhance locomotor responses to novelty, saline, amphetamine, and MK-801. Behav Brain Res, 84:47-55.

Barger SW, Basile AS. (2001) Activation of microglia by secreted amyloid precursor protein evokes release of glutamate by cystine exchange and attenuates synaptic function. J Neurochem 76:846-854.

Behrends JC, Ten Bruggencate G. (1993) Cholinergic modulation of synaptic inhibition in the guinea pig hippocampus in vitro. J Neurophysiology 69:626-629.

Berg L, McKeel DW, et al. (1998) Clinicopathologic studies in cognitively healthy aging and Alzheimer disease. Arch Neurol 55:326-335.

Berg L, Miller JP, et al. (1988) Mild senile dementia of the Alzheimer type. 2. Longitudinal assessment. Ann Neurol 23:477-484.

Berg L, Miller JP, et al. (1992) Mild senile dementia of the Alzheimer type. 4. Evaluation of intervention. Ann Neurol 31:242-249.

Berg L, Morris JC (1994) Diagnosis. In: Alzheimer disease. Terry RD, Katzman R, Bick KL, eds. Raven Press, New York.

Bookstein FL, Green WDK. (1992) Edge information at landmarks in medical images. In Visualization in Biomedical Computing (RA Robb, Ed.) pp. 242-258. SPIE 1808.

Bookstein FL. (1978) The Measurement of Biological Shape and Shape Change. Vol 24. Springer-Verlag: Lecture Notes in Biomathematics, New York.

Borenstein M, Cohen J. (1988) Statistical Power Analysis: A Computer Program. L. Erlbaum Assoc, NJ.

Burke WJ, Miller JP, et al. (1988) Reliability of the Washington University Clinical Dementia Rating (CDR). Arch Neurol 45:31-42.

Burns A, Rossor M, et al. (1999) The effects of donepezil in Alzheimer's disease – results form a multinational trial. Dement Geriatr Cogn Disord 10:237-244.

Choi DW. (1988) Glutamate neurotoxicity and diseases of the nervous system. Neuron 1:623-634.

Christensen GE, Rabbitt RD, Miller MI. (1994) 3D brain mapping using a deformable neuroanatomy. Physics in Medicine and Biology 39:609-618.

Christensen GE, Rabbitt RD, et al. (1995) Topological Properties of Smooth Anatomical Maps. Kluwer Academic Publishers.

Corey-Bloom J, Anand R, Veach J, for the ENA 713B352 Study Group (1998) A randomized trial evaluating the efficacy and safety of ENA 713 (rivastigimine tartrate), a new acetylcholinesterase inhibitor, in patients with mild to moderately severe Alzheimer's disease. Int J Geriatr Psychopharm 1:55-65.

Csernansky JG, Hamstra J, et al. (2004) Correlations between antemortem hippocampal volume and neuropathology in AD subjects. Alz Disease Assoc Disorders. In press.

Csernansky JG, Joshi S, et al. (1998) Hippocampal morphometry in schizophrenia by high dimensional brain mapping. Proc Nat'l Acad Sci 95:11406-11411.

Csernansky JG, Wang L, et al. (2000) Early DAT is distinguished from aging by high-dimensional mapping of the hippocampus. Neurology 55:1636-1643.

Cullen WK, Suh YH, Anwyl R, Rowan MJ (1997) Block of LTP in rat hippocampus in vivo by beta amyloid precursor protein fragments. Neuroreport 8:3213-3217.

Dann R, Hoford J, Kovacic S, Reivich M, Bajcsy. (1989) Evaluation of elastic matching systems for anatomic (CT, MR) and functional (PET) cerebral images. J Comp Assisted Tomogr 13:603-611.
Davis KL, Thal LJ, et al. (1992) A double-blind, placebo-controlled multicenter study of tacrine for Alzheimer's disease. N Engl J Med 327:1253-1259.
Ditzler K. (1991) Efficacy and tolerability of memantine in patients with dementia syndrome: A double-blind, placebo-controlled study. Arzneimittelforschung 42:904-913.
Dutar P, Nicoll RA. (1988) Classification of muscarinic responses in hippocampus in terms of receptor subtypes and second messenger systems. J Neuroscience 8:4212-4224.
Erdo SL, Schafer M. (1991) Memantine is highly potent in protecting cortical cultures against excitotoxic cell death evoked by glutamate and N-methyl-D-aspartate. Eur J Pharmacol 198:215-217.
Farlow MR, Gracon SI, et al. (1992) A controlled trial of tacrine in Alzheimer's disease. JAMA 268:2523-2529.
Farlow MR, Lahiri DK, Poirier J, Davignon J, Schneider L, Hui SL (1998) Treatment outcome of tacrine therapy depends on apolipoprotein genotype and gender of the subjects with Alzheimer's disease. Neurology 50:669-677.
Farlow MR, Tariot PN, et al. (2003) Memantine/donepezil dual therapy is superior to placebo/donepezil therapy for treatment of moderate to severe Alzheimer's disease. Neurology 60 (Suppl 1):A412.
Feldman H, Gauthier S, et al. (2001) A 24-week, randomized, double-blind study of donepezil in moderate to severe Alzheimer's disease. Neurology 57:613-620.
Folstein MF, Folstein SE, McHugh PR. Mini-Mental State. (1975) A practical method for grading the cognitive state of patients for the clinician. J Psychiatric Res 12:189-198.
Forstl H, Sahakian B (1993) Thalamic radiodensity and cognitive performance in mild and moderate dementia of the Alzheimer's type. J Psychiatry Neurosci 18:33-37.
Fox NC, Cousens S, Scahill R, Harvey RJ, Rossor MN. (2000) Using serial registered brain magnetic resonance imaging to measure disease progression in Alzheimer disease: power calculations and estimates of sample size to detect treatment effects. Arch Neurol 57: 339-344.
Fox NC, Crum WR, et al. (2001) Imaging of onset and progression of Alzheimer's disease with voxel-compression mapping of serial magnetic resonance images. Lancet 358: 201-205.
Fox NC, Freeborough PA. (1997) Brain atrophy progression measured from registered serial MRI: validation and application to Alzheimer's disease. J Magn Reson Imaging 7: 1069-1075.
Fox NC, Freeborough PA, Rossor MN. (1996) Visualization and quantification of rates of atrophy in Alzheimer's disease. Lancet 348:94-97.
Frankiewicz T, Potier B, et al. (1996) Effects of memantine and MK-801 on NMDA-induced currents in cultured neurons and on synaptic transmission and LTP in area CA1 of the rat hippocampal slices. Br J Pharmacol 117:689-697.
Frautschy SA, Baird A, Cole GM (1991) Effects of injected Alzheimer b-amyloid cores in rat brain. Proc. Natl. Acad. Sci. USA 88:8362-8366.
Freeborough PA, Fox NC. (1998) Modeling brain deformations in Alzheimer's disease by fluid registration of serial 3D MR images. J Comput Assist Tomogr 22: 838-843.
Freedman M, Oscar-Berman M. (1989) Spatial and visual learning deficits in Alzheimer's and Parkinson's disease. Brain Cogn 11:114-126.
Geinisman Y, Disterhoft JF, et al. (2000) Remodeling of hippocampal synapses after hippocampus-dependent associative learning. J Comp Neurol 417:49-59.
Gomez-Isla T, Price JL, et al. (1996) Profound loss of layer II entorhinal cortex neurons occurs in very mild Alzheimer's disease. J Neuroscience 16:4491-4500.
Grenander U, Miller MI, Christensen G. (1992) Deformable anatomical databases using global shape models. In Proc. Cooperative Working Group on Whole Body 3-D Electronic Imaging of the Human Body. Crew System Ergonomics Information Analysis Center - Wright Patterson Air Force Base (3/9-11).
Grenander U, Miller MI. (1994) Representations of knowledge in complex systems. J Royal Statistical Soc Bull 56:549-603.
Gundersen HJ, Jensen EB. (1987) The efficiency of systematic sampling in stereology and its prediction. J Microsc 147:229-63.

Gundersen HJ, Jensen EB, Tandrup T (1997) The optical rotator. J Microsc 186:108-20.
Haller JW, Banerjee A, et al. (1997) 3D hippocampal morphometry by high dimensional tranformation of a neuroanatomical atlas. Radiology. 202:504-510.
Harkany T, Abraham I, et al. (2000) β–amyloid neurotoxicity is mediated by a glutamate-triggered excitotoxic cascade in rat nucleus basalis. Eur J Neuroscience 12:2735-2745.
Hyman BT, Damasiao AR, VanHoesen GW, Barnes CL. (1984) Alzheimer's disease: Cell-specific pathology isolates the hippocampal formation. Science 225:1168-1170.
Hyman BT, Van Hoeren GW, Damasio AR (1987) Alzheimer's disease: glutamate depletion in the hippocampal perforant pathway zone. Ann Neurol 22:37-38.
Ikeda M, Tanabe H, et al. (1994) MRI-based quantitative assessment of the hippocampal region in very mild and moderate Alzheimer's disease. Neuroradiology 36:7-10.
Ikezu T, Luo X, et al. (2003) Amyloid precursor protein-processing products affect mononuclear phagocyte activation: Pathways for sAPP- and Aβ-mediated neurotoxicity. J Neurochem 85:925-934.
Iosifescu DV, Shenton ME, Warfield SK, Kikinis R, Dengler J, Jolesz FA, McCarley RW (1997) An automated registration algorithm for measuring MRI subcortical brain structures. NeuroImage 6:13-25.
Jack CR, Peterson RC, O'Brien PC, Tangalos EG. (1992) MR-based hippocampal volumetry in the diagnosis of Alzheimer's disease. Neurology 42:183-188.
Jack CR, Petersen RC, et al. Rate of medial temporal lobe atrophy in typical aging and Alzheimer's disease. (1998) Neurology 51:993-999.
Jarvis B, Figgitt DP. (2003) Memantine. Drugs Aging 20:465-476.
Jobst KA, Smith AD, et al. (1994) Rapidly progresive atrophy of medial temporal lobe in Alzheimer's disease. Lancet 343:829-930.
Joshi S, Miller MI, Grenander U. (1997) On the geometry and shape of brain sub-manifolds. IJPRAI (Special Issue).
Kawas C, Clark CM, Farlow MR, et al. (1999) Clinical trials in Alzheimer's Disease: Debate on the use of placebo contols. Alz Dis Assoc Disord 13:124-129.
Killiany RJ, Moss MB, et al. (1993) Temporal lobe regions in magnetic resonance imaging identify patients with early Alzheimer's disease. Arch Neurol 50:949-954.
Kilpatrick GJ, Tilbrook GS. (2002) Curr Opin Investig Drugs 3:798-806.
Kim SH, Price MT, Olney JW, Farber NB. (1999) Excessive cerebrocortical release of acetylcholine induced by NMDA antagonists is reduced by GABAergic and alpha2-adrenergic agonists. Molecular Psychiatry 4:344-352.
Kim J, Fanselow MS (1992) Modality-specific retrograde amnesia of fear. Science 256:675-677.
Knapp MJ, Knopman DS, et al. (1994) A 30-week randomized controlled trial of high-dose tacrine in patients with Alzheimer's disease. J Am Med Assoc 271:985-991.
Knopman D, Kahn J, Miles S. (1998) Clinical research designs for emerging treatments for Alzheimer disease: moving beyond placebo-controlled trials. Arch Neurol 55:1425-1429.
Knopman D, Morris JC. (1997) An update on primary drug therapies for Alzheimer's disease. Arch Neurol 54:1406-1409.
Kraemer HC, Thiemann S. (1987) How Many Subjects? Sage Publications, New York.
Laakso MP, Partanen K, et al. (1996) Hippocampal volumes in Alzheimer's disease, Parkinson's disease with and without dementia, and vascular dementia: an MRI study. Neurology 46:678-681.
Laird NM, Ware JH (1982) Random-effects models for longitudinal data. Biometrics 38:963-974.
Lipton SA, Rosenberg PA. (1994) Excitatory amino acids as a final common pathway for neurologic disorders. New Eng J Med 330:613-621.
Marvanova M, Lakso M, et al. (2001) The neuroprotective agent memantine induces brain-derived neurotrophic factor and trkB expression in rat brain. Mol Cell Neurosci 18:247-258.
Mathalon DH, Sullivan EV, Rawles JM, Pfefferbaum A. (1993) Correction for head size in brain-imaging measurements. Psychiatry Research: Neuroimaging 50:121-139.

Mattson MP, Barger SW, et al. (1993) β-amyloid precursor protein metabolites and loss of neuronal Ca^{2+} homeostasis in Alzheimer's disease. Trends Neurosci 16:409-414.
McKhann G, Drachmann D, et al. (1984) Clinical diagnosis of Alzheimer's disease: Report of the NINCDS-ARDDA work group under the auspices of Department of Health and Human Services Task Force on Alzheimer's disease. Neurology 34:939-944.
M'Harzi M, Gieules C, Palou A-M, Oberlander C, Barzaghi F (1997) Ameliorating effects of RU 47213, a novel oral and long-lasting cholinomimetic agent, on working memory impairment in rats. Pharmacol Biochem Behav 56:663-668.
Miguel-Hidalgo JJ, Alvarez XA, Cacabelos R, Quack G. (2002) Neuroprotection by memantine against neurodegeneration induced by β-amyloid (1-40). Brain Res 958:210-221.
Miller MI, Banerjee A, et al. (1997) Statistical methods in computational anatomy. Statistical Methods in Medical Research 6:267-299.
Miller MI, Christensen GE, Amit Y, Grenander U. (1993) Mathematical textbook of deformable neuroanatomies. Proc Natl Acad Sci 90:11944-11948.
Miller MI, Hosakari M, Priebe C, Ratnanather JT, Wang L, Gado M, Csernansky JG. (2003) Labeled cortical depth maps quantifying cortical change during aging and DAT. Proc Nat'l Acad Sci USA 100:15172-15177.
Miller MI, Massle A, Ratnanather JT, Botteron K, Csernansky JG. (2000). Bayesian construction of geometrically bases cortical thickness metrics. Neurology 12:676-687.
Miltner FO. (1982) Use of symptomatic therapy with memantine in cerebral coma. I. Correlation of coma stages and EEG spectral patterns. Arzneimittelforschung 32:1268-1270.
Monarch ES, Rick J, Goldstein FC, Hamann SB (1999) Fear conditioning is impaired in early Alzheimer's disease. Soc Neurosci Abst 25:99.
Morris JC. (1993) The Clinical Dementia Rating (CDR): Current version and scoring rules. Neurology 43:2412-2414.
Morris JC, Edland S, Clark C, et al. (1993) The consortium to establish a registry for Alzheimer's Disease (CERAD). Part IV. Rates of cognitive change in the longitudinal assessment of probable Alzheimer's disease. Neurology 43:2457-2465.
Morris JC, Cyrus PA, et al. (1998) Effects of metrifonate on the cognitive, global, and behavioral function of Alzheimer's disease patients: Results of a randomized, double-blind, placebo-controlled study. Neurology 50:1222-1230.
Morris JC, McKeel DW, et al. (1988) Validation of clinical diagnostic criteria for Alzheimer's disease. Ann Neurol 24:17-22.
Morris JC, McKeel DW, et al. (1991) Very mild Alzheimer's disease: Informant-based clinical, psychometric, and pathological distinction from normal aging. Neurology 41:469-478.
Morris JC, Storandt M, et al. (1996) Cerebral amyloid deposition and diffuse plaques in " normal" aging: Evidence for presymptomatic and very mild Alzheimer's disease. Neurology 46:707-719.
Mungas D, Reed BR, Jagust WJ, et al. (2002) Volumetric MRI predicts rate of cognitive decline related to AD and cerebrovascular disease. Neurology 59:867-873.
Murphy DGM, DeCarli CD, et al. (1993) Volumetric magnetic resonance imaging in men with dementia of the Alzheimer's type: correlations with disease severity. Biol Psych 34:612-621.
Ohno M, Kishi A, Watanabe S. (1996) Effect of cholinergic activation by physostigmine on working memory failure caused in rats by pharmacological manipulation of hippocampal glutamatergic and 5-HTergic neurotransmission. Neurosci Lett 217:21-24.
Parks JK, Smith TS, et al. (2001) Neurotoxic Aβ peptides increase oxidative stress in vivo through NMDA-receptor and nitric-oxide-synthase mechanisms, and inhibit complex IV activity and induce a mitochrondrial permeability transition in vitro. J Neurochem 76:1050-1056.
Pearlson GD, Harris GJ, et al. (1992) Quantitative changes in mesial temporal volume, regional cerebral blood flow, and cognition in Alzheimer's disease. Arch Gen Psych 49:402-408.

Phillps RG, LeDoux JE (1992) Differential contribution of amygdala and hippocampus to cued and contextual fear conditioning. Behav Neurosci, 106:274-285.
Price JL, Morris JC. (1999) Tangles and plaques in nondemented aging and preclinical Alzheimer's disease. Ann Neurol 45:358-368.
Raskind SL, Peskind ER, et al. (2000) Galantamine in AD: A 6-month, randomized, placebo-controlled trial with a 6-month extension. Neurology 54:2261-2268.
Ratnanather JT, Priebe CE, Miller MI (2003) Semi-automated segmentation of cortical subvolumes via hierarchical mixture modeling. In: Medical Imaging 2003: Image Processing (eds. Sonka M and Fitzpatrick JM). Proc SPIE 5032:1602-1612.
Reisberg B, Doody R, Stoffler A, Schmitt F, Ferris S, Mobius HJ and the Memantine Study Group (2003) Memantine in moderate-to-severe Alzheimer's disease. New England J Medicine 348:1333-1341.
Rogers SL, Farlow MR, et al. (1998) A 24-week, double-blind, placebo-controlled trial of donepezil in patients with Alzheimer's disease. Neurology 50:136-145.
Rogers SL, Friedhoff LT (1996) The efficacy and safety of donepezil in patients with Alzheimer's disease: Results of a US multicentre, randomized, double-blind, placebo-controlled trial. Dementia 7:293-303.
Rosen WG, Mohs RC, Davis KL. (1984) A new rating scale for Alzheimer disease. Am J Psychiatry 141:1356-1364.
Samuels SC, Davis KL (1998) Experimental approaches to cognitive disturbance in Alzheimer's disease. Harvard Rev Psychiatry 6:11-22.
Scheltens P, Leys D, et al.. (1992) Atrophy of the medial temporal lobes on MRI in "probable Alzheimer's disease and normal aging: diagnostic value and neuropsychological correlates. J Neuro Neurosurg Psych 55:967-972.
Shenton ME, Kikinis R, et al. (1992) Abnormalities of the left temporal lobe and thought disorder in schizophrenia. N Engl J Med 327:604-612.
Sheridan RD, Sutor B. (1990) Presynaptic M1 muscarinic cholinoceptors mediate inhibition of excitatory synaptic transmission in the hippocampus in vitro. Neurosci Lett 108:273-278.
Squire LR, Zola-Morgan S. (1991) The medial temporal lobe memory system. Science 253:1380-1386.
Steckler T, Sahgal A. (1995) The role of serotonergic-cholinergic interactions in the mediation of cognitive behaviour. Beh Brain Res 67:165-199.
Tariot PN, Farlow MR, et al. (2004) Memantine treatment in patients with moderate to severe Alzheimer Disease who are already receiving donepezil. J Am Med Assoc 291:317-324.
Thal LJ, Schwartz G, Sano M, et al. (1996) A multicenter double-blind study of controlled-release physostigmine for the treatment of symptoms secondary to Alzheimer's disease. Neurology 47:1389-1395.
Thompson PM, MacDonald D, Mega MS, Holmes CJ, Evans AC, Toga AW. (1997) Detection and mapping of abnormal brain structure with a probabilistic atlas of cortical surfaces. J Comp Asst Tomography 21:567-581.
Umbriaco D, Garcia S, Beaulieu C, Descarries L. (1995) Relational features of acetylcholine, noradrenaline, serotonin and GABA axon terminals in the striatum radiatum of adult rat hippocampus (CA1). Hippocampus 5:605-620.
Venkatesan R, Haacke EM. (1997) Role of high resolution in magnetic resonance (MR) imaging: Applications fo MR angiography, intracranial T1-weighted imaging, and image interpolation. Int J Imaging Syst Technol 8:529-543.
Wang L, Swank J, et al. (2003) Changes in hippocampal volume and shape across time distinguish dementia of the Alzheimer type from healthy aging. NeuroImage 20:667-682.
Weller M, Finiels-Marlier F, Paul SM. (1993) NMDA receptor-mediated glutamate toxicity of cultured cerebeller, cortical and mesenencephalic neurons: Neuroprotective properties of amantidine and memantine. Brain Res 613:143-148.
West MJ, Slomianka L, Gundersen HJG. (1991) Unbiased stereological estimation of the total number of neurons in the subdivisions of the rat hippocampus using the optical fractionator. Anat Record 231:482-497.

Wilcock G, Wilkinson D. (1996) Galanthamine hydrobromide: Interim results of a group comparative, placebo controlled study of efficacy and safety in patients with a diagnosis of senile dementia of the Alzheimer type. Neurobiol Aging 17:S144.
Wyss JM, van Groen R. (1989) Development of the hippocampus. In: The Hippocampus - New Vistas (Eds: V. Chan-Palay, C. Kohler) Neurology and Neurobiology, Vol. 52, Alan R. Liss, Inc. pp. 1-17.
Zola-Morgan S, Squire L. (1993) Neuroanatomy of memory. Annual Rev Neurosci 16:547-563.